Implementation of Vibration Suppression on an Aircraft Wing Using Velocity Feedback Controller

Asst. Prof. Dr. Ahmed A. Ali
Baghdad University-Engineering College
Email: Dr.Ahmed.ali@coeng.uobaghdad.edu.iq
Prof. Dr. Hussain Y. Mahmood
Baghdad University-Engineering College
Email:Hussain_Yousif2001@yahoo.com
Mahmood Wael Saeed
Ph.D. student-Applied Mechanics
Baghdad University-Mechanical Engineering
Email:mahmoodwael@rocketmail.com

ABSTRACT:-
Active vibration control had been presented as an effective tool for vibration suppression of an aerobatic aircraft wing (CH650). In this work both numerical and experimental tests were performed for tested wing. Total wing was modeled in finite element software (ANSYS V.15) in which velocity feedback controlling method was integrated. Two materials were tested to compare the effectiveness of controller for each material. Scaled model was fabricated in laboratory with two different spars' materials which were [0/90] composite and aluminum foam. In experimental part piezoelectric transducers were used as actuators and sensors to perform controlling action with totally integrated controller circuit within (LABVIEW 2015). Results showed that using of velocity feedback controlling method can add more stability to the tested wing where 83% of wing's settling time was eliminated with using aluminum foam as a manufacturing material for wing's spars.

Key words:- Active vibration control, Velocity feedback, Aircraft wing, LABVIEW.

1. Introduction:-
Vibration in any mechanical system is undesirable issue due its dangerous manifold on any part of the structure, so it is important to safe the vibrated structure from collapse to prevent disaster results especially if the structure is in direct contact with humans like aircrafts, trains and buildings, .etc. Active regulating technique has become precious tool aside from inactive method over the past decades for suppression the operational vibrations of mechanical structures. The main objective of a controlling circuit is to eliminate the responses that were formulated by different disturbances or by primary energy sources. Many researchers worked on attenuation of vibration in many mechanical structures where in references **[1, 3]**, vibration attenuation for an aerobatic aircraft wing was introduced numerically for two different manufacturing materials. Classical PID controller was also

utilized to achieve the controlling action. In reference **[2]** a comparison between classical PID controller and velocity feedback performance was presented for actively suppression of vibration generated during flutter case of typical delta wing with first mode of vibration tested for three manufacturing materials. About 75% of the overall wing tip vibration was suppressed by using PI controller. While about 93% of wing's vibration was mitigated with direct velocity feedback method for wing manufactured from aluminum foam. Experimental and numerical tests were carried out in reference **[4]** for typical delta wing under first mode of vibration. Excellent enhancement in structure's vibrational performance was achieved. Acceleration feedback was used as a controller for active vibration attenuation of an unmanned aircraft wing as presented in reference **[5]**.

Authors in reference **[13]** introduced a remediable controller for actively controlling of system vibration. Full scaled multilayer composite airplane wing was used in his works as a tested model. The controller was consisted from multiple components with multiple input/ output paths. Micro fiber composite (MFC) actuator was used because of its ability to be sticking on curved surfaces, position of MFC actuators and sensors were estimated by using genetic algorithm technique. Experimental results were showed excellent performance of this controller. Authors in reference **[12]** studied the effect of introducing Integral Consensus Control (ICC) for controlling of structural vibration. Beam built in from one end and free from the other was used to estimate the effectiveness of the introduced controlling method via finite element analysis for many types of excitations. Results show that ICC led to improving system stability for any intended mode. Radek Matušů, et al**.** in reference **[15]** studied an airplane's wing for vibration control, tested wing has an obliquely shape. In order to increase or in another word enhance PID regulators' stability, authors works on estimating all reachable method for increasing stability of PID. The main thought of the explained technique was built according to on Tan's method for estimating of (optimal) settling down for both PID and PI regulators or increase steadiness of PI regulators by aims of presenting the steadiness environment by either P-I plane or P-I-D space. Rearrangement of the currently used technique by utilizing of sixteen part plants instead of sixteen Kharitonov plants provides further increasing in steadiness of mentioned regulator. Authors in reference **[17]** mentioned that (PD) Proportional-derivative regulator and proportional-integral-derivative (PID) regulator were the most famous controlling techniques in most engineering projects. However, not enough results in attenuation of oscillation by using mentioned type of regulator. Reference **[11]** introduced an approach for executing modal

analysis of free active flexible multi body systems. Two types of sensing tools were utilized; first one in collocated and second type was non-collocated. Numerical representation had been performed to check the performance of proposed technique. Multiple inputs/outputs loop was used with PID regulator for satisfying approach. Authors in reference **[16]** studied the ability of two types of controllers in vibration suppression of composite plate used for aero elastic analysis. Derivative of velocity and proportional feedback was used as controllers with PZT as sensors and actuator. Authors worked on satisfy best distribution of actuators to get best controlling effect. Different ply angle was tested for mentioned controllers to show their effect on un damped natural frequencies and overall responses. Analytical and modal analysis of tested model was formulated by MATLAB codes; no experimental tests had been presented.

In the current work vibration suppression of scaled (CH650) aircraft wing was tested experimentally and numerically. This work is invoked for enhancing the vibrational behavior of the mentioned wing. Passive vibration control was achieved by testing two manufacturing materials for wing's spars. Then active vibration control was performed by utilizing velocity feedback (VF) method as a vibration controller. The coupling between active and passive controlling methods leads to further enhancement on the overall free response of the tested wing.

2. FE MODEL

The concept of piecewise discretization or dividing a complex object into simpler pieces is one of the oldest logical concepts known to man, when trying either to construct a complex shape or to understand an enigmatic phenomenon. Aerobatic aircraft wing was modeled closely to real one, this wing is mainly containing two spars each one is located at 25% of chord length from both leading and trailing edge respectively**, [18].** NACA 0015 is the airfoil section of mentioned wing with 8 ribs along wing's length, distance between each rib is 0.375m which is continuously exceeded until the 8^{th} rib at which wing length reaches to 3m. Tapering ratio of modeled wing was 0.51 in X & Y coordinates (coordinate system used for modeling process); chord length of first airfoil section was 1.6 m. Each spar was of 3.3m total length which was distributed as 3m wing's length inside wing's body passing through the eight ribs with similar tapering ratio in Y direction only. The remaining 0.3m of spars length was used for fixation of wing with airplane body. In ANSYS CH650 wing was modeled with scale of 1/3 real wing dimensions, where by using [kp] command 78 keypoint was modeled to form airfoil shape as shown in **Fig.1**

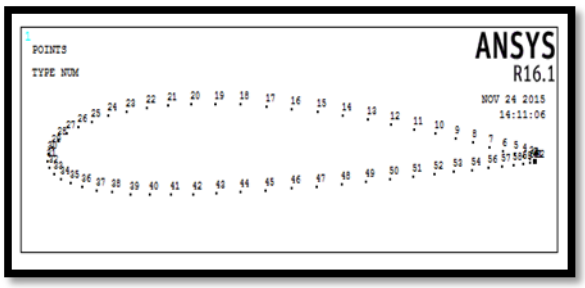

Fig. 1 Outlines of NACA 0015 airfoil

Through these keypoints splines were drawn via [splin] command to create border of airfoil's border as shown in **Fig.2, [7].**

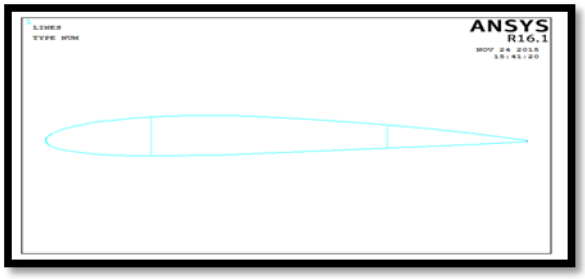

Fig.. 2 Airfoil of tested wing

Then by using [AL] command a completed area of airfoil section was created as shown on **Fig.3**.

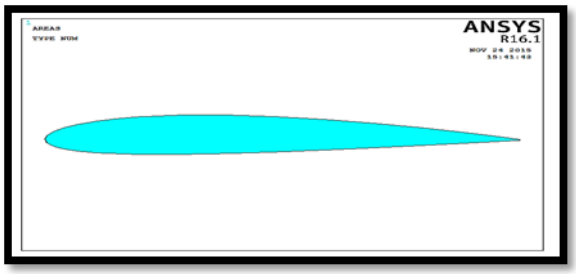

Fig.. 3 2D Airfoil section

Front and back spars were formulated firstly by line connecting between two keypoints of airfoil points as shown in **Fig.2** for both first and back spars respectively. These two lines are converted directly to area when [vext] command was used. ANSYS APDL [vext] command was applied with offsetting of 3m in z direction and 0.2m in x direction to generate wing's body as a volume with mentioned tapering ratios, after that 6 rectangular area was modeled starting from 2nd rib until 7th, benefits of these rectangular areas were to generate the remaining ribs where via [asbv] command, the total wing's body was divided into seven volumes each one with extension of 0.375m. But as the real wing is internally hollow, [vdele] command was used to delete volumes only with keeping all covering areas. Inner construction of the wing is shown in **Fig.4** with dimension of each part. In **Fig.5** total wing is shown with skin as a final result of previously mentioned steps. Wing was modeled by a fast and simple method where in which small numbers of commands was used to simplify modeling and in the same time modeling of studied wing precisely. The suitable type of elements used in the discretization of the aircraft wing structure is the shell element. Shell is defined as an object which, for the purpose of analysis may be considered as the materialization of a curved surface **[8].**

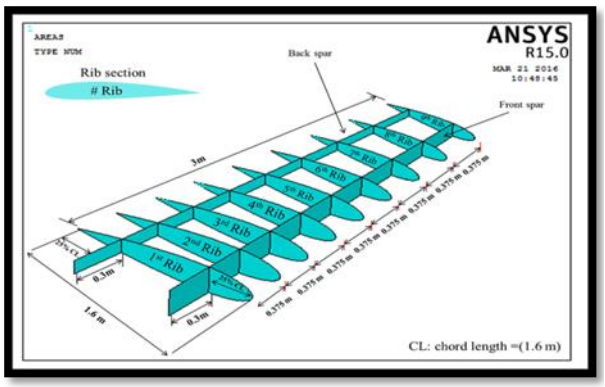

Fig. 4 Inner construction of wing

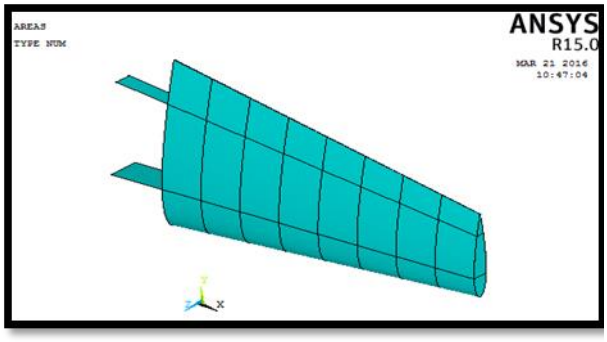

Fig. 5 Total wing model

SHELL181 is appropriate for analyzing thin to thick shell structure. It has translations in the x, y and z directions and rotations about the x, y, and z-axes therefore six degrees of freedom at each node and it is four node elements. SOLID5 was used to model piezoelectric transducers where it has a 3-D magnetic, thermal, piezoelectric, electric and structural field capability with limited coupling between the fields. The element has 8 nodes. Each node has u_x, u_y and u_z (displacements along x, y, and z axis respectively), in addition to temperature, voltage and scalar magnetic potential as degrees of freedom.

3. VELOCITY FEEDBACK (VF) CONTROLLER

Equation of motion for multi degree of freedom system is presented by:

$$M\ddot{\delta} + K\delta = f + Bq \quad \text{..... (1)}$$

Where M, K, f, q, B, δ, $\dot{\delta}$ and $\ddot{\delta}$ are mass, stiffness, force, control force, influence matrix, displacement, velocity and acceleration sets matrices respectively. Force of control produced by VF is presented by:

$$q = -c\dot{\delta} \quad \text{..... (2)}$$

(c) is the controller gain and $\dot{\delta}$ set of velocity measurements, here structural damping was omitted to present the full effect of controller purely on the studied structure.so by combination of both **Eq. (1)** and **(2)** will lead to:

$$M\ddot{\delta} + Bc\dot{\delta} + K\delta = f \quad \text{..... (3)}$$

By comparing **Eq. (3)** with the general equation of motion $M\ddot{\delta} + C\dot{\delta} + K\delta = f$ form it clear to be noted that with controller the [C] matrix which presents viscous damping which is increased due to controlling force **[9]**. Block diagram of VF control is shown in **Fig.6.** Firstly initial displacement of 0.001m was applied on CH650 wing's tip. static analysis was performed in order to create transient initial condition to be applied by using initial condition ([ic]) ANSYS command, where from the first step the displacement of all structure's nodes were collocated in matrix with single column and nth row, nth is the total node counts. The extracted displacement will lead to make the structure oscillating freely. It is important to be noted that the number

of nodes included in [ic] command must be equal to the total number of nodes that forming meshed structure. A comparison between free, control OFF and control ON is then performed to decide which material was the best and which controller was the effector.

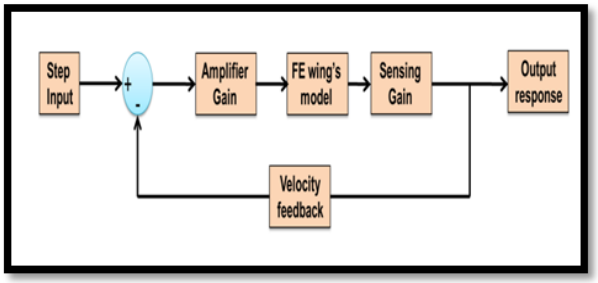

Fig. 6 Block diagrams VF controller

4. EXPERIMENTAL MODEL

Wing was constructed totally from 2021 aluminum for ribs, skin and spars path. It is important to keep all dimensions of fabricated wing similar to numerical model as near as possible to satisfy logical comparison between experimental and numerical results. Consequently, the nine NACA 0015 ribs shown in **Fig.7** of tested wing were cut via high precision SKYCNC-2412 plasma machine-Germany this type of CNC is programmable with 3D milling tool charger, 3D high-speed machining features with a very smooth cut edges. High, complex series of processing was performed on tested model due to Airfoil's curved shape. This series of processing adds more accuracy on transferring numerical model to real model. Starting from airfoil section, file of tested model was exported from ANSYS©environment with extension [.IGES] to be processed with AutoCAD©2016 where by which file of [.DWG] extension was exported to CorelDraw©2016 program in which smoothing process for airfoil section was applied and all required dimensions were adjusted. File with [.ESP] extension was then exported to be programmed in CNC language. Scaled chord length of 1.6m real length was selected and cut for NACA0015 airfoil.

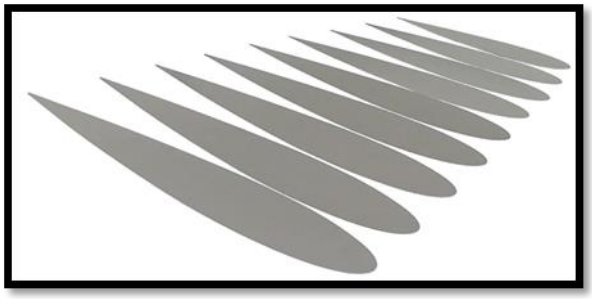

Fig. 7 NACA 0015 airfoil –Aluminum

In addition, spar's path was formulated by upper and lower half-rectangular section as shown in **Fig.8** with mentioned dimensions in which also the tip spar edge is presented. Both upper and lower spar path edges was constructed to formulate trapezoidal spar shape in which one can insert different spar's material with similar dimension as will be presented later. Similar steps of real wing fabrication were followed with each part of studied wing until total wing structure completed, after that full inner wing construction was collocated as in which one can notice a clear view on spars path and positions of ribs on spars and positions of connecting points. Skinning process was perform after that with a difficult of estimating drilling position on both chip and skinning plate respectively. Then total

wing which is presented in **Fig.9** was completed by skinning all its inner ribs and spars.

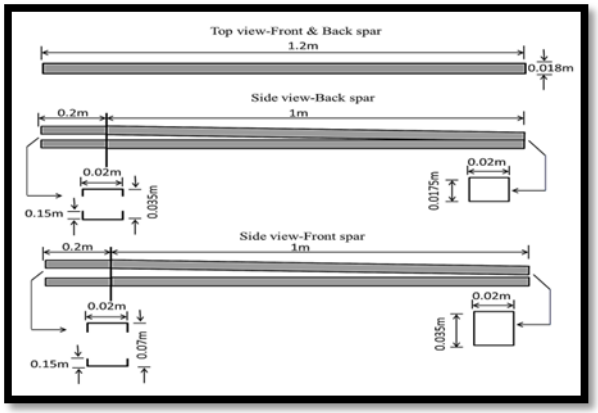

Fig. 8 Dimensions of spars

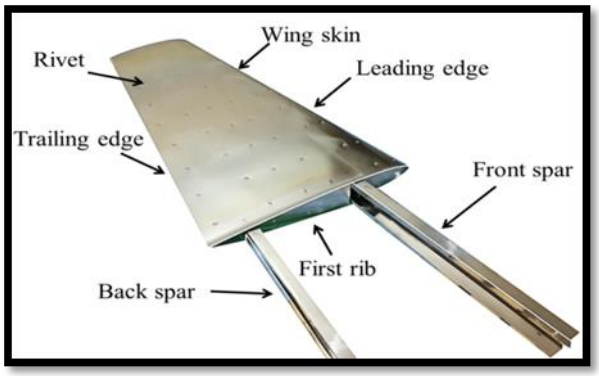

Fig. 9 Total wings

5. PREPARATION OF SPARS

5.1 Aluminum Foam Spars

Spars made from aluminum foam was cut with dimensions shown in **Fig.10** for both front and back spar, closed cell foam produced by {Shanxi putai Co. Ltd. Beijing} with material properties as presented in **Table .1**, **Fig.10** show spars of aluminum foam.

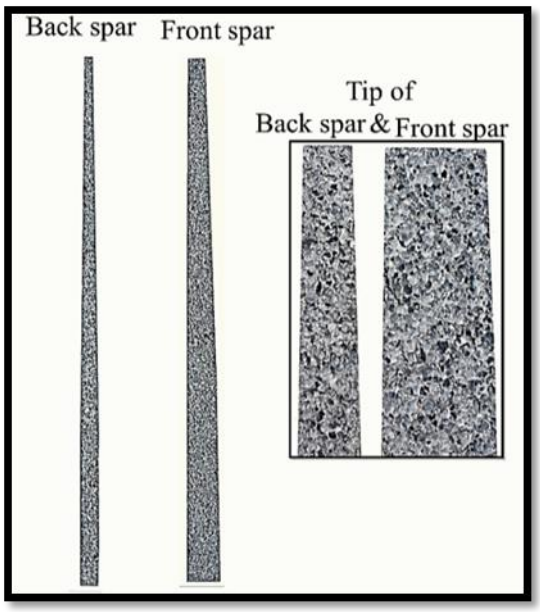

Fig. 10 Spars of AL- foam

5.2 Composite Spars

Both front & back spars were manufactured from [0/90] composite material. Steps of the manufacturing process are listed below:

1- Raw materials (glass fibers, resin, hardener and thickener) for producing a composite material were prepared, besides fiber scissor and brushers. Since it is important to keep manufacturing process in safe side all required safety instruments (eye protect glass, gloves and mask) were used during process. **Fig.11** shows all required materials and instruments for composite manufacturing.

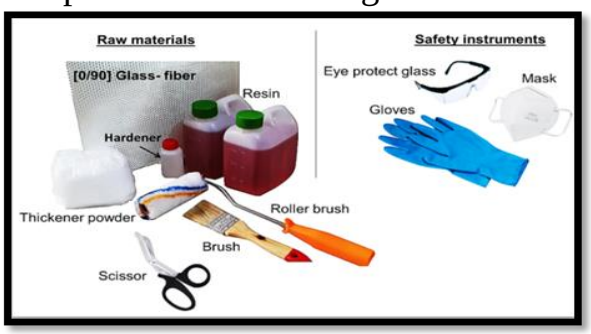

Fig. 11 Raw materials & safety instruments for manufacturing composite material.

2- Two aluminum molds were fabricated for both front and back spars respectively as shown in **Fig.12** these molds are coated with a thin layer of separator liquid before starting in manufacture process, this layer will facilitate taking off models from molds.

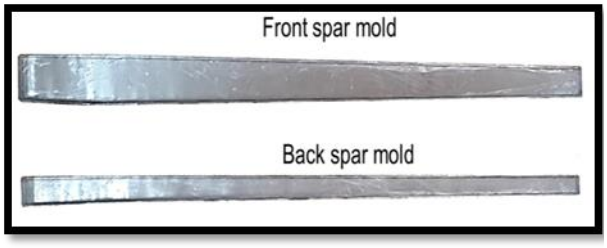

Fig.12 Aluminum molds for producing composite spars

3- Manufacturing steps are listed in **Fig.13a** where in steps 1&2 fiber cutting and fitting are presented. First resin layer is presented in step 3, which followed by first glass fiber layer in step four, then repeating the process in step 5 until completing spar model as presented in step 6. After drying up of resin with fiber, the spars were extracted from mold and processed by grinder to remove any growths from the spar's edge as stated in step 7. **Fig.13b** shows composite spars in mold while complete spars were presented in **Fig.13c**.

(a) (b) (c)

Figure. 13 Manufacturing process of composite Spars

6. EXPERIMENTAL WORK

Generally; experimental work was divided into two parts; free response recording and active vibration control. Each part will be described as follow:

1. Uncontrolled response was sensed by using accelerometer (4366- Brüel & Kjær).Chassis NI-9178 with embedded analog input NI 9215 module (data acquisition system) was used to convert sensed signal from analog to digital signal. Free Responses were recorded and processed in LABVIEW. For enhancing sensed signal, filter from signal processing pallet was used in the experimental work. **Fig.14** shows experimental presentation for sensing the free responses.

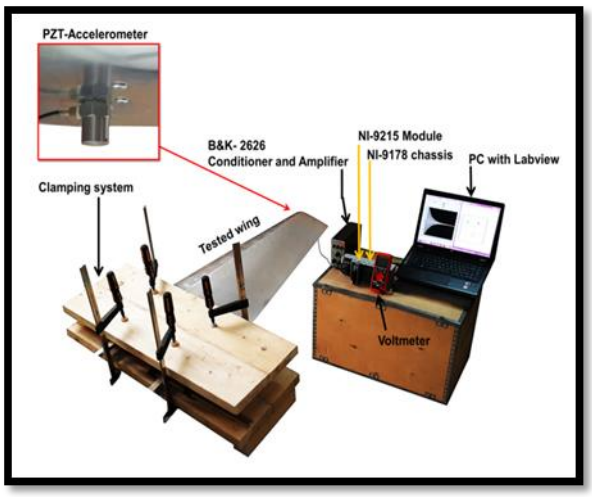

Fig. 14 Recording of free responses

2- Controlled response for two smart wings, first wing was CH650 (composite and aluminum foam spars). Responses were measured experimentally as mentioned previously for the comparison with numerically measured responses. The smart tested wings were equipped with piezoelectric patches to act as actuators, where CH650 wing was with four embedded piezoelectric transducers. The piezoelectric actuators (**PPA-1001)** are bonded onto wing skin using special piezoelectric adhesive. Sensor is glued in the z direction of the lower wing's skin**.** It is important to use high speed data acquisition system to ensure fast recording, processing and controlling action without any delay and within short duration, so (PCI e 9321) Express data acquisition was used for transmission sensed signal to controller circuit in LABVIEW and then export it to signal amplifier (Trek® model 2205.USA) high voltage amplifier. Most devices used in present work are programmable, so as will introduce in next section LABVIEW program was used to build controlling circuit and specify its regulating specifications. The tip displacements responses of tested wings are obtained by calibration between the sensor voltages and tip displacements U_Z which is programmed as an equation within LABVIEW. Controlled responses for tested wings are presented in **Fig.15**.

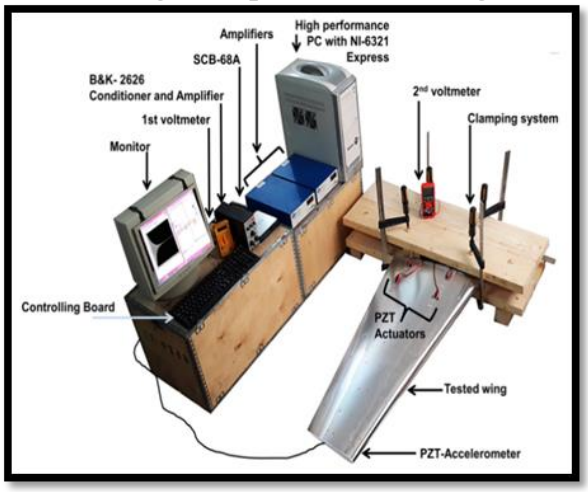

Fig. 15 Experimental active vibration control system

7. MATERIAL PROPERTIES

Material properties of Aluminum and composite of [0/90] is listed in **Table .1**. Also material properties of PPA-1001 piezoelectric transducer produced by (MIDE) are listed in table.1. Mechanical properties of both symmetric laminated glass epoxy composite [0/90] and Aluminum were calculated according to ISO 6892-1:2009E by Iraqi Central Organization for Standardization and Quality Control (COSQC), **[10], [14]** .Also all physical and electrical properties of piezoelectric transducers are supported

from (MIDE Co. for PPA-1001) **[6], 2016**. Wing's dimensions are listed in **Tabel .2**

8. RESULTS AND DISCUSSION

Results of free as well as forced vibrations and active control vibrations are investigated for tested smart aircraft wings are presented in this chapter. Firstly, the natural frequencies and mode shapes are introduced with and without piezoelectric patch as well as the effects of changing the position of piezoelectric are presented. Also, the free vibration (displacement response in time domain) is shown as passive control to select the best location for PZT. Finally, active control vibration is applied for free vibration by using VF controller to reduce the undesired vibrations. Mode shapes of CH650 wing with composite Spars, without piezoelectric transducers and mode shapes of CH650 wing of composite Spars with and without piezoelectric transducers are presented in **Figs. 16 & 17** respectively. By comparison **Figs. 16 &17** and **Figs. 18 & 19** it is easy to notice that composite spars effect on decreasing natural frequencies of aluminium structure by 5.5 Hz this decreasing is due high density of composite spars relative to aluminium one where that acts on increasing mass which in opposite proportion with natural frequency. **Figs. 18 & 19** present mode shapes of CH650 wing foam spar without PZT and with PZT respectively. By comparing foam modes with previous AL & composite modes it is notable decreasing in natural frequency by 4 Hz was noticed in changing aluminium spar with foam spar increasing in natural frequency of composite spars by 2.4 Hz this decreasing in natural frequency is due to relatively low foam density in comparison with composite mass. VF responses are presented in **Fig. 20** in which controlled responses of composite wing using velocity feedback controlling technique with gain of 0.5, 0.7, 1 and 1.2 are stated. 68% decreasing in in overall settling time was performed by this method. Best enhancement is settling time was satisfied at gain of 1.2. High improvement in wing's response was satisfied by VF method with low serving energy (voltage), this feature makes VF more suitable to be used with relatively big structures. This enhancement in settling time with VF is due to adding more damping on tested structure. Total comparison between VF gains and their corresponding voltages are presented in **Fig. 21.** Maximum actuation voltage was applied at VF with gain 1.2. **Fig. 22** shows overall responses comparison between wing's responses with VF velocity for spars made from aluminium foam. Based on high performance of VF techniques that noticed in previously tested spars one can be utilized this economic method to produce an optimal controlled response for aluminium foam spars. Velocity feedback controlling technique was carried out with gain of 0.5, 0.7, 1 and 1.2 as presented in **Figs. 23 & 24** where at gain of 1.2 more

than (83%) of time required to settle vibrated wing was eliminated. Experimental responses for both composite spars and aluminum foam spars are presented in **Fig. 25~ 26.** Experimental results show a good agreement with numerically represented responses. Most of differences were because of disturbances effect on both electrical devices and data transmission cables.

9. CONCLUSIONS

Some important conclusions and results can be obtained from this study as follows:

1. The three dimensional finite element model proposed can predict accurately the free vibration and controlling response of tested aircraft wings for different material properties and different controlling type.

2. Dynamic response of a tested wings can be effectively suppressed with the application of the piezoelectric elements, When the piezoelectric elements are placed near the fixed end of the plate ,where relatively high strains occur, the control effects improve faster that when the piezoelectric elements are placed in the relatively low strain area.

3. Velocity feedback controller can effectively suppressed free vibration of wing with aluminum foam spars better than the wing with composite spars.

References

1. Ahmed Abdul-hussain Ali, “Stability Improvement of an Unmanned Aerial Vehicle's Wing using Active Vibration Control”, International Journal of Computer Applications, Vol. 157, No. 10, January 2017.
2. Ahmed Abdul-hussain Ali, Hussain Yousif Mahmood, and Mahmood Wael Saeed, “A Comparison between Velocity Feedback and Proportional-Integral- Derivative [PID] Performance In Active Vibration Control”, Journal of Vibration Analysis, Measurement, and Control, Vol. 4, No. 1, 2016.
3. Ahmed Abdul-hussain Ali, Hussain Yousif Mahmood, and Mahmood Wael Saeed, “Active Vibration Control of Aircraft Wing Using Piezoelectric Transducers”, International Journal of Scientific & Engineering Research, Vol. 7, No. 5, May 2016.
4. Ahmed Abdul-hussain Ali, Hussain Yousif Mahmood, and Mahmood Wael Saeed, “Experimental and numerical vibration attenuation for delta wing using PI controller”, Al-Nahnrain journal for engineering sciences, April, 2017
5. Ahmed Abdul-hussain Ali, Mahmood Wael Saeed, “Active Vibration Suppression of Aerobatic Aircraft Wing by Acceleration Feedback Controller”, International Journal of Computer Applications, Vol. 157, No. 10, January 2017.
6. Data sheet, 2016, MIDE Co. Ltd., PPA-1001- PPA-series.
7. Dimensions sheet of NACA0015, NASA, and Available from: http://airfoiltools.com/airfoil/details?airfoil=naca0015-il.

8. Flugg W., 1967, “Stresses in Shell”, Springer-Verlag, 4th edition, New York.
9. Levent Malgaca, 2007, “Integration of Active Vibration Control Methods with Finite Element Models of Smart Structure”, Thesis of Degree of Doctor Mechanical Engineering, Middle East university, Turkey.
10. Material test, Aluminum, Iraqi Central Organization for Standardization and Quality Control (COSQC).
11. M. Bratland, B. Haugen, and T. Rolvag, “Modal analysis of active flexible multibody systems”, Computers & Structures, Vol. 89, No. 9-10, pp. 750–761, 2011.
12. Omidi E, Mahmoodi SN., 2015, “Vibration suppression of distributed parameter flexible structures by Integral Consensus Control”, Journal of Sound and Vibration, Vol. 364, PP. 1–13.
13. Prakash S, Renjith Kumar TG, Raja S, Dwarakanathan D, Subramani H, Karthikeyan C., 2016, “Active vibration control of a full scale aircraft wing using a reconfigurable controller”, Journal of Sound and Vibration, Volume 361, PP. 32–49.
14. R.C. HiBLER, 2008, “Mechanics of Materials”, Pearson prentice hall.
15. Radek Matušů, Prokop R, 2015, “Robust Stabilization of Oblique Wing Aircraft Model Using PID Controller” , 8th IFAC Symposium on Robust Control Design ROCOND, Bratislava, Vol. 48, No. 14, PP. 8-11
16. Song Z, Li F., 2012, “Active aeroelastic flutter analysis and vibration control of supersonic composite laminated plate”, Composite Structures, Vol. 94, No. 2, PP. 702–13.
17. Thenozhi S, Yu W., 2014, “Stability analysis of active vibration control of building structures using PD / PID control”. Engineering Structures, Vol. 81, No. 15, PP. 208–18.
18. Zenith Aircraft Company, 2015, “Design & construction Kit”, USA.

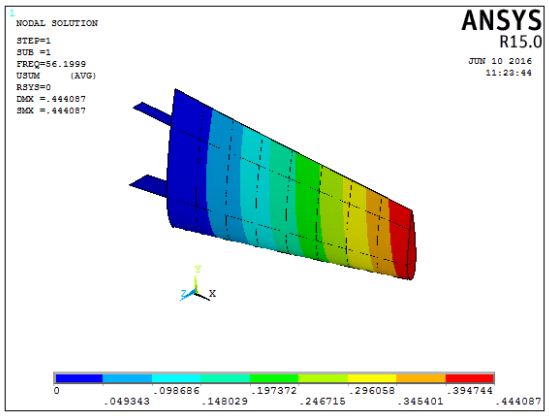

a. 1st mode

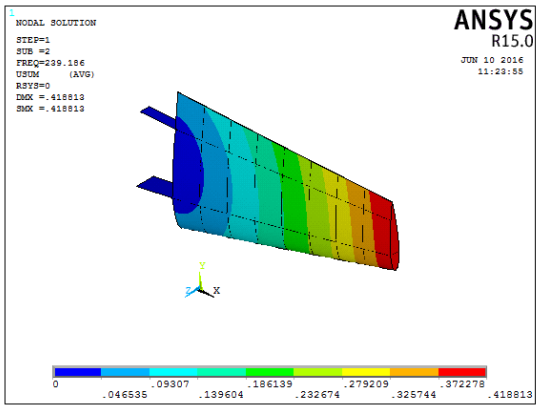

b. 2nd mode

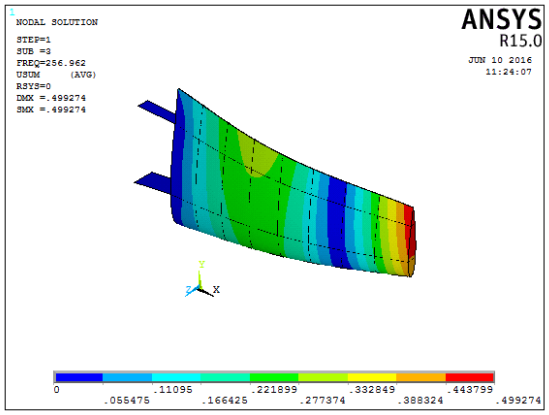

c. 3rd mode

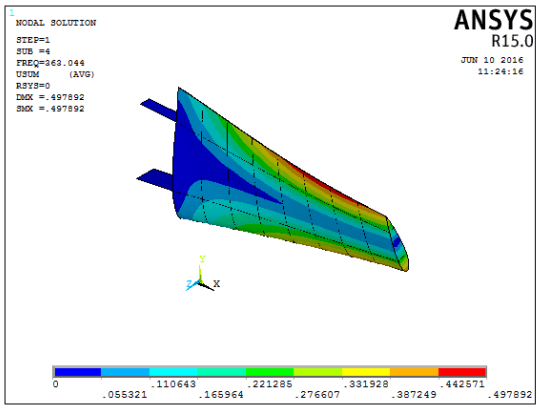

d. 4th mode

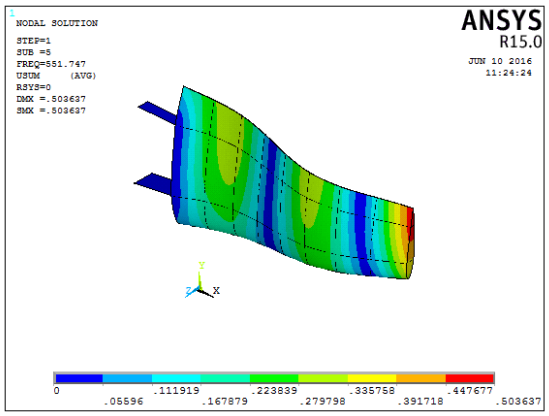

e. 5th mode

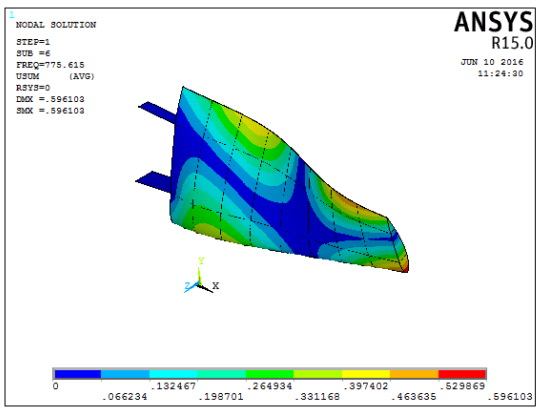

f. 6th mode

Fig. 16 Mode shape of CH650 composite spars wing

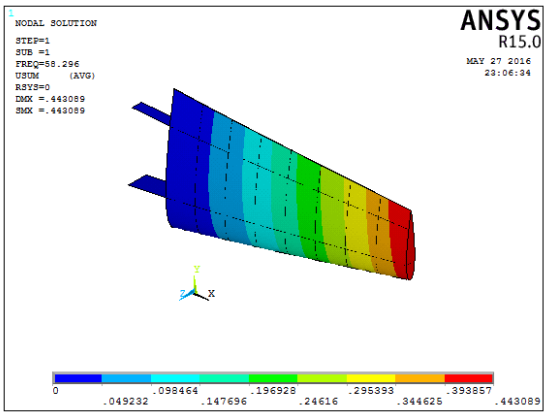

a. 1st mode

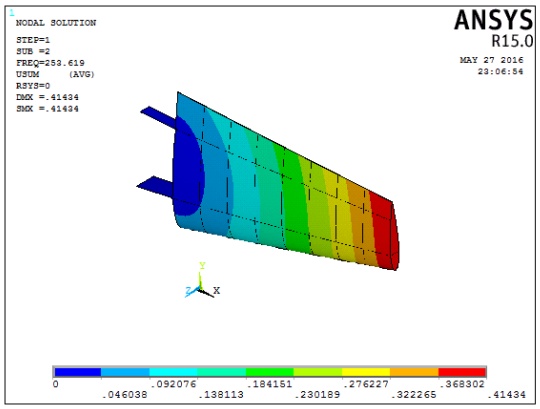

b. 2nd mode

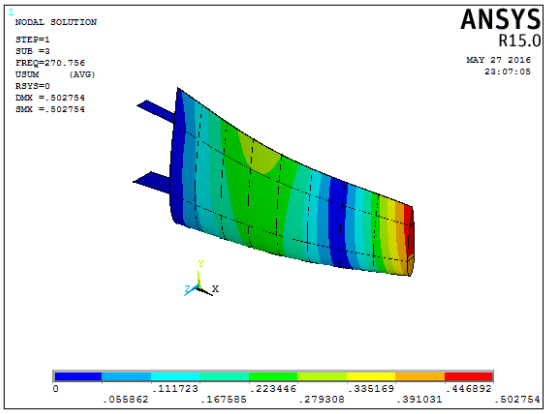

c. 3rd mode

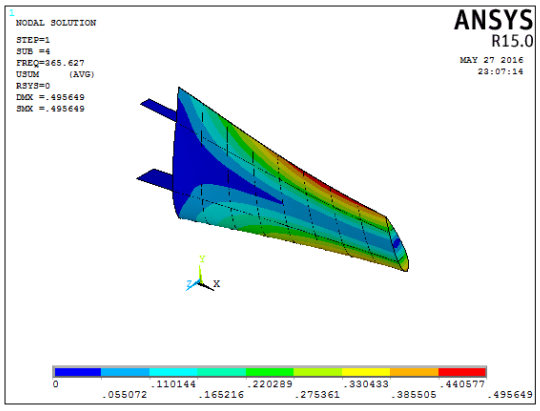

d. 4th mode

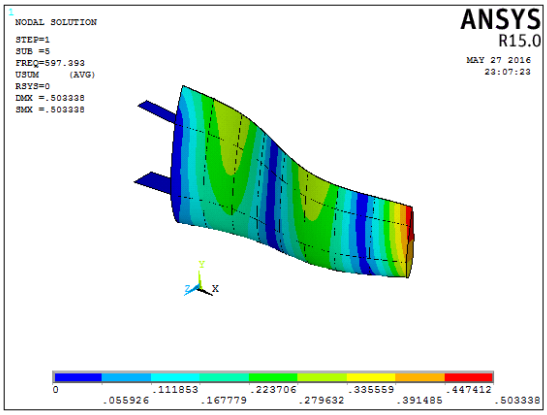

e. 5th mode

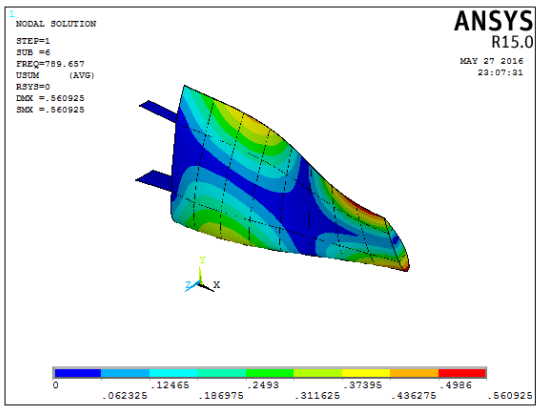

f. 6th mode

Fig. 17 Mode shape of CH650 Foam spars wing

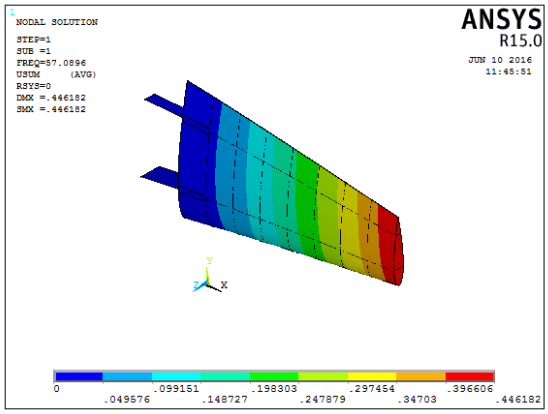

a. 1st mode

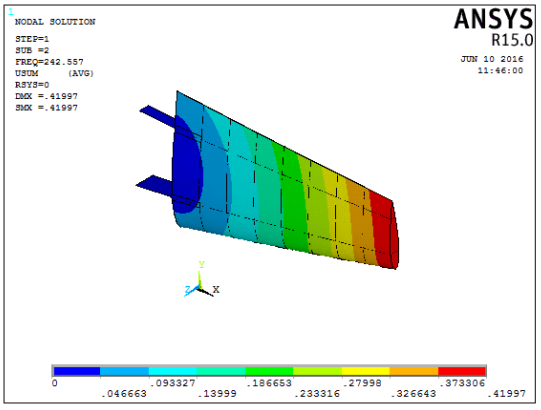

b. 2nd mode

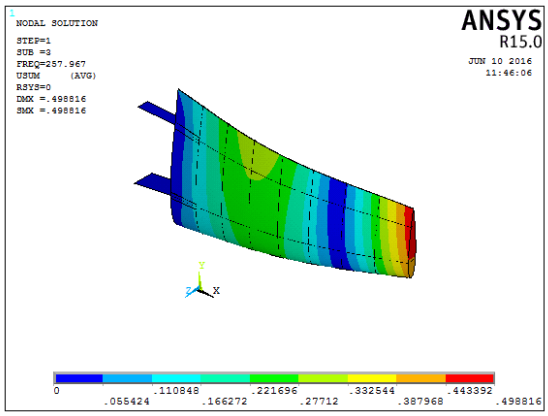

c. 3rd mode

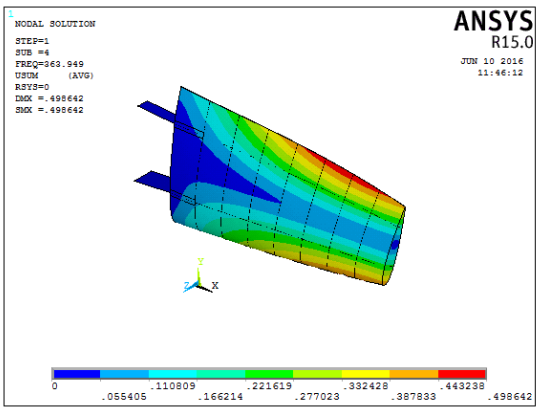

d. 4th mode

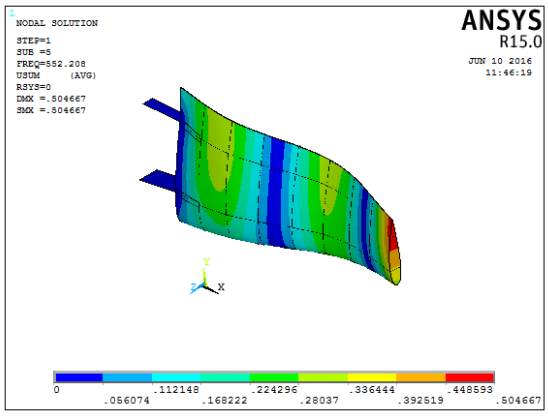

e. 5th mode

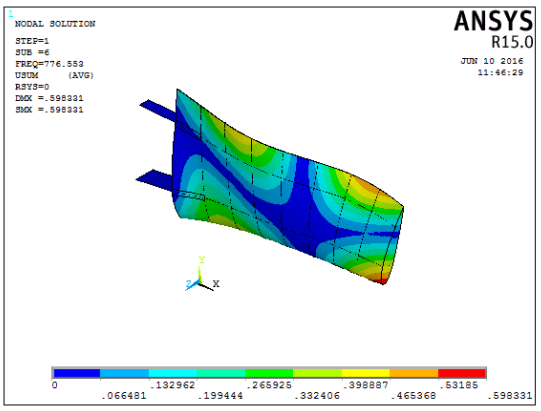

f. 6th mode

Fig. 18 Mode shape of CH650 composite spars wing with PZT

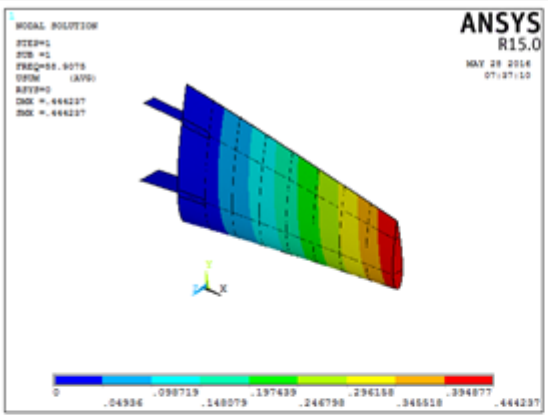

a. 1st mode

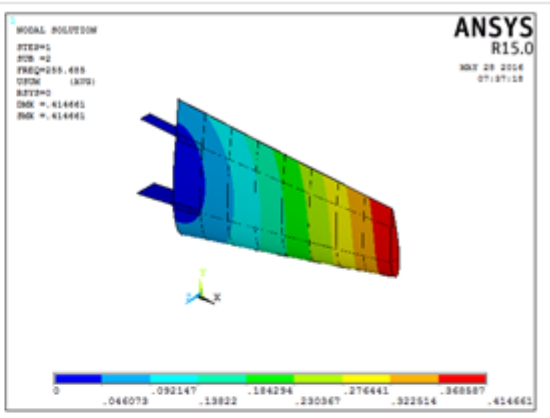

b. 2nd mode

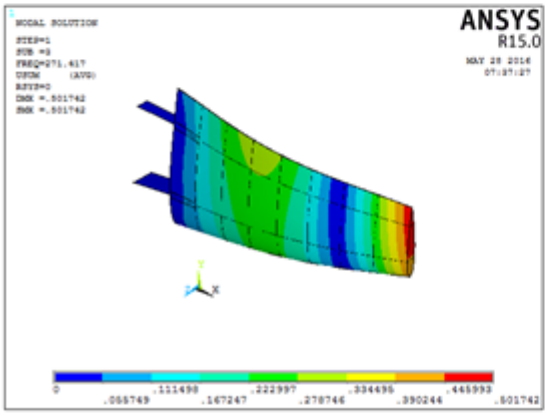

c. 3rd mode

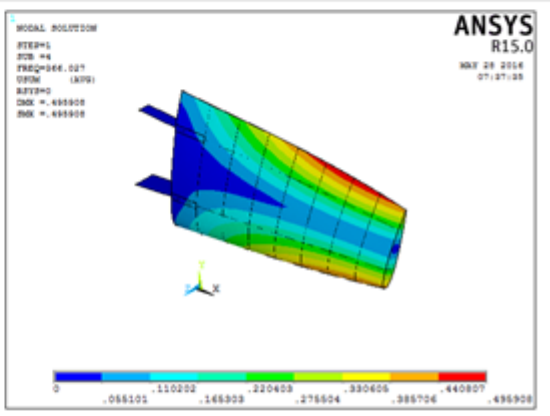

d. 4th mode

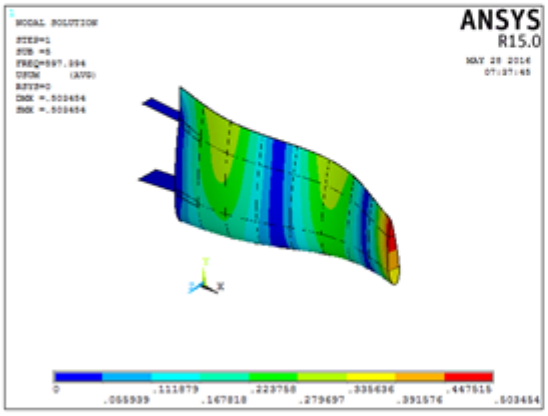

e. 5th mode

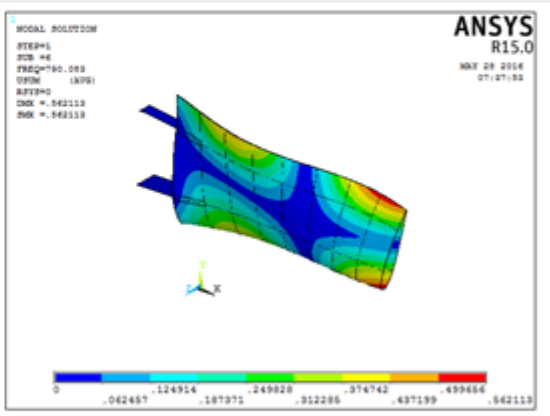

f. 6th mode

Fig. 19 Mode shape of CH650 foam spars wing with PZT

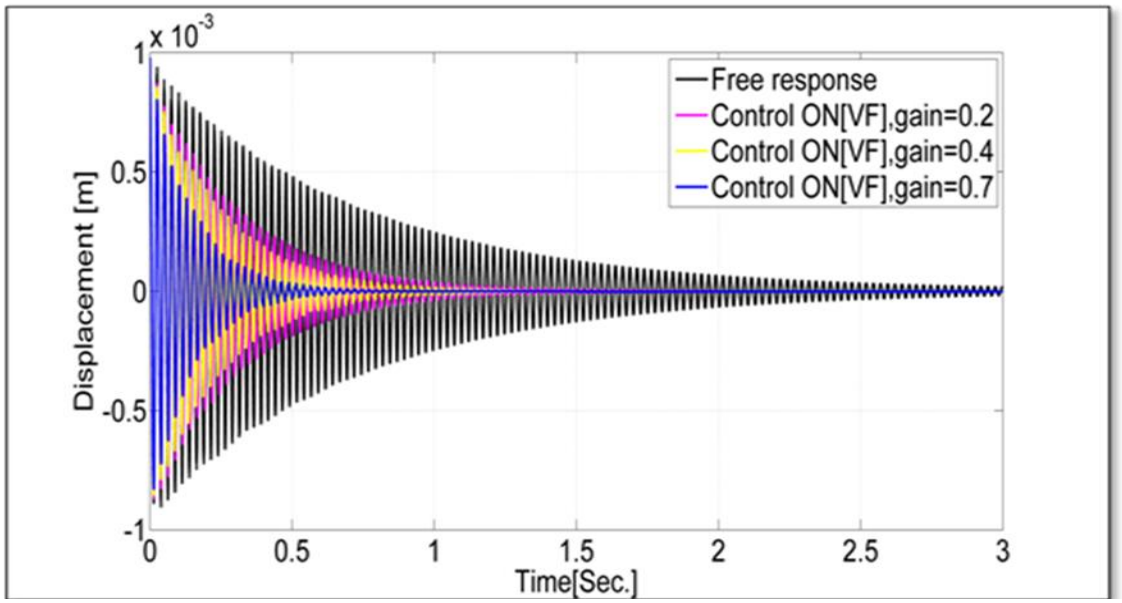

Fig. 22 Comparison of responses with VF controller for Aluminum foam spars wing

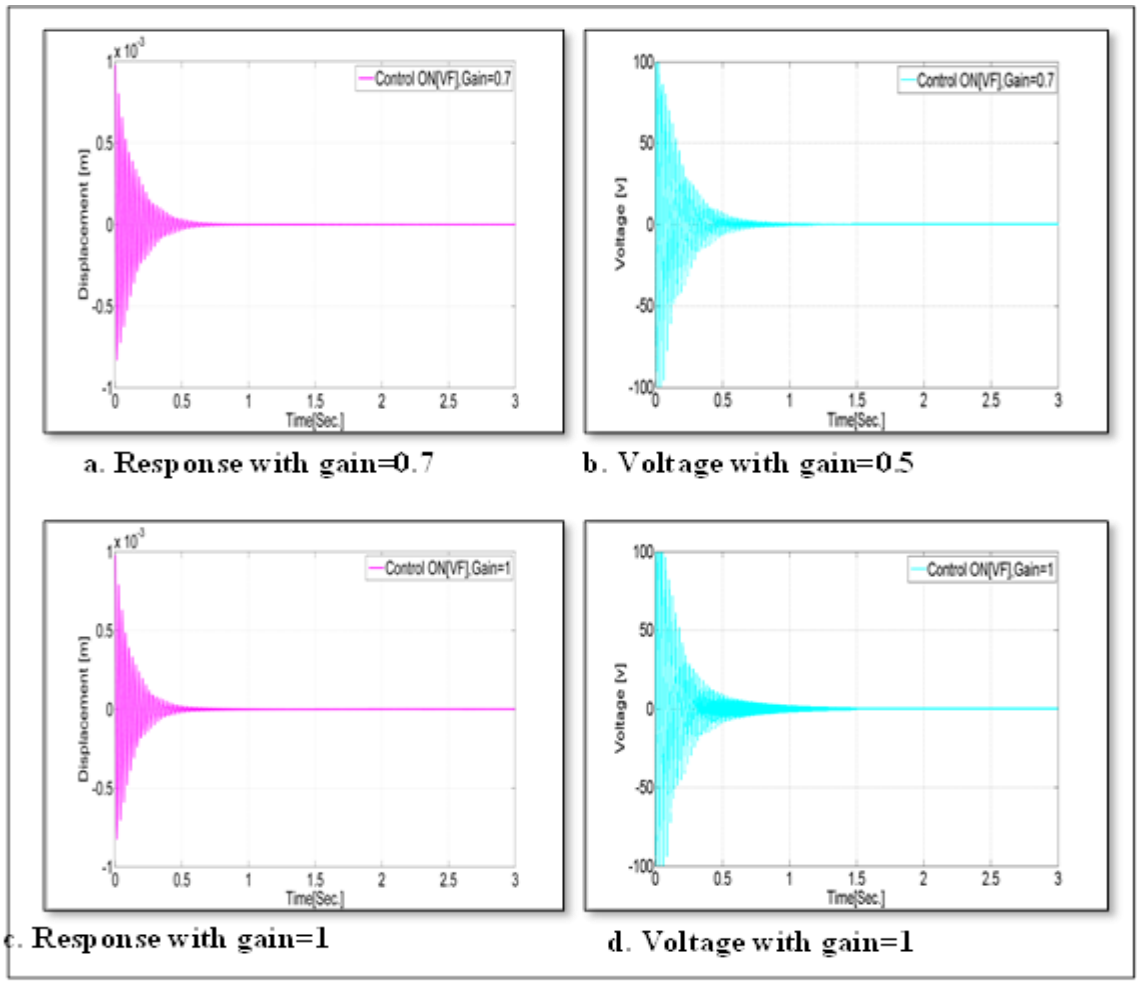

Figure. 23 Response of CH650 wing with Aluminium foam Spars

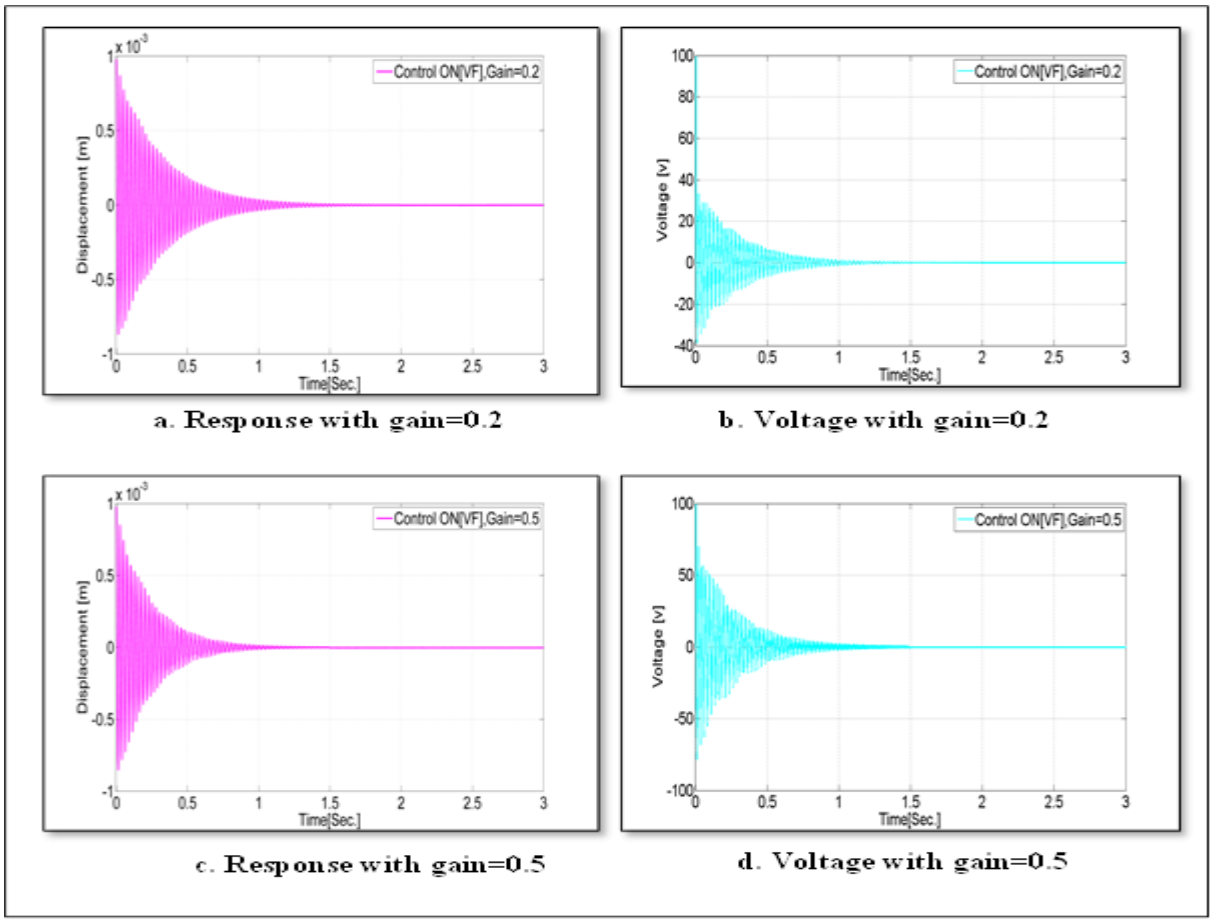

a. Response with gain=0.2 b. Voltage with gain=0.2

c. Response with gain=0.5 d. Voltage with gain=0.5

Figure. 24 Response of CH650 wing with Aluminium foam Spars

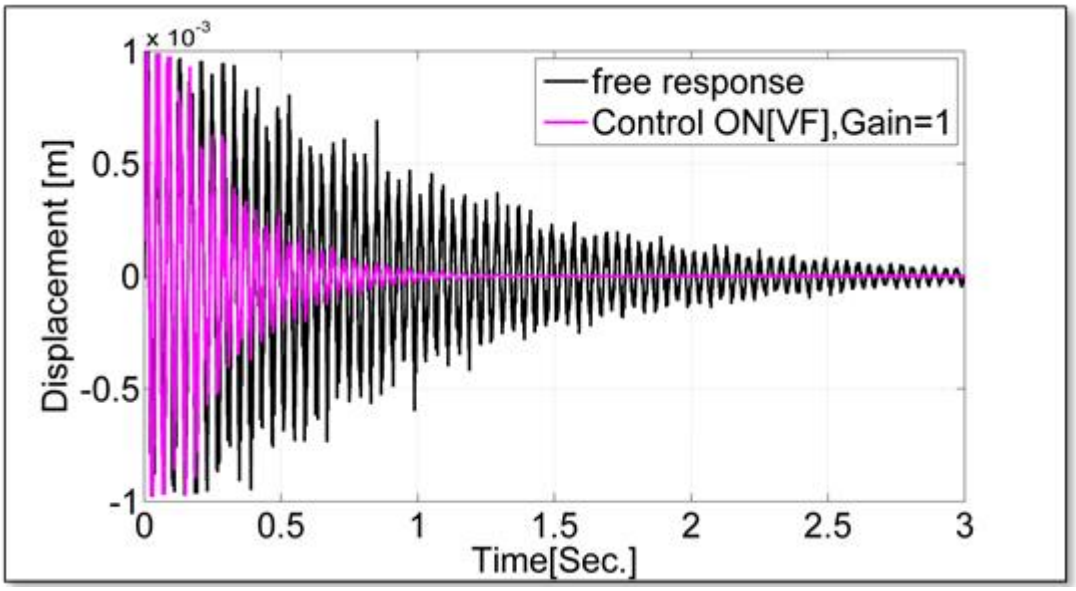

Fig. 25 Experimental comparison of responses for aluminium foam spars wing with VF controller

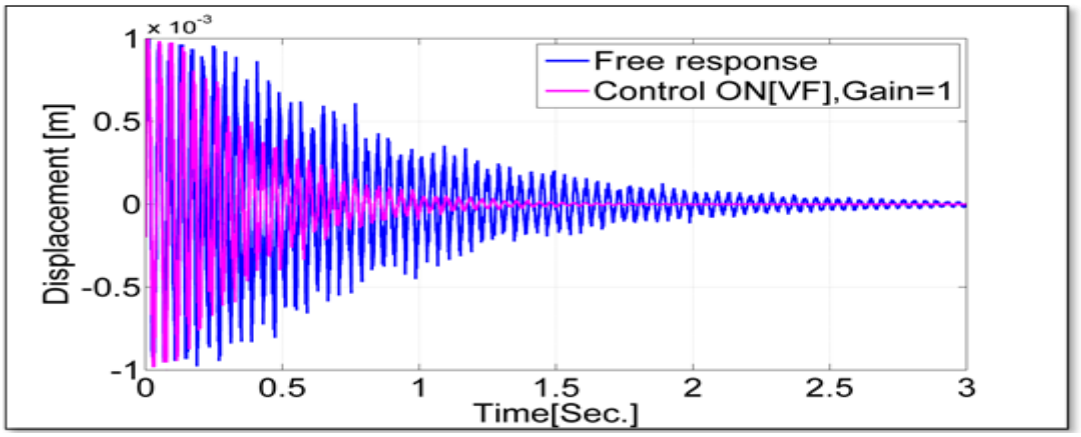

Fig. 26 Experimental comparison of responses for composite spars wing with VF controller

Table .1 Material properties

Total wing span (m)	1.2
Wing area (m^2)	0.432
Aspect ratio	2.3148
Taper ratio	0.51
Mean aerodynamic chord (m)	0.4
Root chord (m)	0.528
Tip chord (m)	0.26928

Table .2 Dimensions of tested Wing

PPA-1001 Piezoelectric actuator	Epoxy-glass composite structure
ρ =7350 kg/$\mathbf{m^3}$ Piezoelectric strain matrix (C/$\boldsymbol{m^2}$) E31 = 6.5× $\mathbf{10^9}$ E33 = 23.3× $\mathbf{10^9}$ E15 = 17× $\mathbf{10^9}$ Elastic stiffness matrix (N/$\mathbf{m^2}$) C11 = 12.6 C12 = 7.95 C13 = 8.41 C33 = 11.7 C44 = 2.33 Dielectric matrix (F/m) e11 = 1.503×$\mathbf{10^{-9}}$ e22 = 1.503×$\mathbf{10^{-9}}$	ρ =1830 kg/m^3 Ex = 40.51 GPa Ey = 13.96 GPa Ez = 13.96 GPa Gxy = 3.1 GPa Gyz = 1.55 GPa Gxz = 3.1 GPa νxy = 0.22 νyz = 0.11 νxz = 0.22

تمثيل تخميد الاهتزاز على جناح طائرة باستخدام منظم ارجاع السرعة

الاستاذ المساعد الدكتور أحمد عبدالحسين علي
جامعة بغداد- كلية الهندسة
الاستاذ الدكتور حسين يوسف محمود
جامعة بغداد- كلية الهندسة
محمود وائل سعيد
طالب دكتوراه - ميكانيك تطبيقي
جامعة بغداد- كلية الهندسة

الخلاصة

تم تقديم طريقة التخميد الفعال كأداة فعالة لتخميد اهتزاز جناح طائرة (سي اتش)650 . تم اجراء اختبارات نظرية وعملية للنموذج المدروس حيث تم تمثيل الجناح باستخدام برنامج المحاكاة (ANSYS V.15) والذي تم فيه برمجة الية عمل منظم ارجاع السرعة. تم اختبار مادتين مختلفتين في صناعة سارية الجناح وذلك لغرض اجراء مقارنة لكفاءة المنظم لكل مادة. تم بناء نموذج الجناح عمليا في المختبر من مادتين مختلفتين لسارية الجناح وهما (90/0) مواد مركبة ورغوة الالمنيوم. تم استخدام المواد الذكية كمتحسسات ومولدات اثارة مع دائرة سيطرة كاملة في برنامج (LABVIEW 2015).
أظهرت النتائج ان استخدام طريقة ارجاع السرعة تحسن استقرارية الجناح المدروس حيث قد خفضت 83% من زمن استقرار سارية جناح مصنوعة من رغوة الالمنيوم.

الكلمات الرئيسية: طريقة التخميد الفعال, ارجاع السرعة, جناح طائرة, LABVIEW.